Chalcogenide Letters Vol. 18, No. 8, August 2021, p. 481 - 491

Copper-tin-sulphide (CTS) thin films, obtained by a two-electrode electrochemical deposition of metal precursors, followed by soft annealing and sulfurization

D. B. Puzer, I. Nkrumah*, F. K. Ampong, M. Paal, E. A. Botchway, R. K. Nkum, F. Boakye
Department of Physics, Kwame Nkrumah University of Science and Technology, Kumasi, Ghana

CTS thin films have been prepared by soft annealing and sulfurization of electrodeposited Cu-Sn precursors. The stacked elemental layer approach was used to deposit the elemental precursors on an ITO substrate using a two-electrode electrochemical cell, with graphite plate as the counter electrode. The stacked metallic layer was then soft annealed in an Argon atmosphere at 350 °C and subsequently, sulfurized at different temperatures of 500 ^{0}C and 550 ^{0}C for one hour to form CTS films. The films have been characterized by a variety of techniques. From the XRD analysis, the CTS thin films obtained at a sulfurization temperature of 500 ^{o}C showed the coexistence of SnS, Cubic-$Cu_2Sn_3S_7$ and hexagonal-$Cu_4S_{16}Sn_7$ phases. The majority phase was clearly identified as cubic-Cu_2SnS_3, with (111) preferential orientation. For the films sulfurized at 550 ^{o}C, the pattern of prominent peaks showed the presence of the Hexagonal-$Cu_4S_{16}Sn_7$ phase of CTS with preferred orientation along the (202) plane. There were relatively fewer low intensity peaks assigned to the secondary phases, indicating an improvement in CTS purity at the higher sulfurization temperature. SEM images of the CTS films show a compact, homogenous morphology, with densely packed grains. The films sulfurized at 550 ^{o}C, showed better homogeneity. EDAX spectra of the sulfurized alloy precursors were consistent with the formation of CTS. The film obtained at the lower sulfurization temperature had two band gaps as a consequence of the mixture of phases present in the sample. The film obtained at the higher sulfurization temperature had an energy band gap of 1.5 eV, which falls within the range of values reported in literature. The present work provides a new synthesis route for the electrodeposition of CTS thin film for device applications.

(Received May 10, 2021; Accepted August 25, 2021)

Keywords: Electrode deposition, Copper-tin sulfide, Thin films

1. Introduction

Copper tin sulphide (CTS), compounds are promising solar absorber materials for the production of cheaper large-scale thin film solar cells, due to the abundance of the constituents in the Earth's crust [1]. CTS is a p-type semiconducting material belonging to an important category of I-V-VI ternary chalcogenide materials. The origin of the p-type conductivity is from the defect formed from vacancies and cation–cation disorder [2]. CTS has a wide range of stability in the Cu-Sn-S system in the chemical potential phase space [3], showing polymorphs such as monoclinic [4], cubic [5], tetragonal [6], triclinic [7], wurtzite [8] and hexagonal structures [9]. The polymorphs have been observed to produce different band gaps due to varied geometric arrangements of the various ions in the structures [9]. Pan et al. [10] have explained that the varying crystal structures portray a semiconducting behaviour which can be attributed to the sulphur atoms packing very closely to the copper-tin metals preventing S-S atoms from bonding directly. Michaelson [11], in a comparative study of CTS reported that the monoclinic phases have relatively fewer defects and recommended their usage in producing high PCEs PV cells. Other properties of CTS, include a high absorption coefficient (10^5 cm^{-1}), an electrical conductivity of 10 Ω^{-1} cm^{-1}, a hole mobility of 80 cm^2 V^{-1} s^{-1}, a hole concentration of 10^{18} cm^3 [1], and a tunable optical band gap ranging from 0.9 – 1.77 eV [12, 13]. Additionally, CTS has an excellent

* Corresponding author: inkrumah.sci@knust.edu.gh

https://doi.org/10.15251/CL.2021.188.481

conductivity (3.43 S/cm at room temperature) [14], making it a suitable material for application in low cost and eco-friendly thin film solar cells. This and other multifunctional applications, such as; a promising p-type thermoelectric material, a potential anode material in lithium ion batteries, among others, has made the ternary CTS semiconductor compound, a feasible material of research interest [15, 16].

Several studies on CTS compound reports a number of factors that could influence its properties including; secondary phases (i.e CuS, SnS Cu_2S, and SnS_2), composition ratio, dopants, grain size, crystal structure, and among others [17, 16, 10]. It is therefore important that studies seek to establish the deposition conditions that produce CTS films with the desired properties.

CTS thin films have been synthesized by several techniques such as; thermal evaporation [18], sputtering [17, 19, 20], spray pyrolysis [21], spin coating [22], chemical bath deposition [23, 24], co-evaporation [25] and electrochemical deposition [12, 26].

Electrodeposition has emerged as a one of the versatile and cost-effective growth technique of metal, metalloid and semiconductor materials [12, 27]. With emphasis on semiconductor growth, the use of either two or three-electrode electrodeposition technique has been effective in the growth of high-performance semiconductor materials.

Of particular interest are its cost effectiveness, low toxicity, high purity, large area deposition, scalability, and room temperature growth. Film properties can be controlled by adjusting electrodeposition parameters like temperature, pH, concentration of electrolyte, and deposition potential [28, 29].

There are two ways to deposit CTS thin films by electrodeposition (ED), either the stacked elemental layer (SEL) approach followed by sulphurization or the single step approach [30]. The former benefits from good metal layer stability and adherence [31]. Common sulphur environments used are hydrogen sulphide gas or sulphur vapour.

Several research papers on the electrochemical deposition of CTS, reveal that most researchers employ the conventional three electrode configuration. The use of a simple two-electrode configuration for electrodeposition of semiconductors is very rare. Echendu et al. [32] carried out a comparative study on using the two-electrode and three-electrode configurations, and concluded that electrochemical deposition of semiconductors in general can equally be carried out using two-electrode system as well as the conventional three-electrode system without compromising the essential qualities of the materials produced. The report further highlights the advantages of the two-electrode configuration in process simplification, cost reduction and removal of a possible impurity source in the growth system, especially as the reference electrode ages.

In the present work, CTS thin films have been prepared by soft annealing and sulphurization of electrodeposited Cu-Sn precursors. The SEL approach is used to deposit the elemental layers on an ITO substrate, using a two-electrode electrochemical cell with graphite as the counter electrode. The soft annealed and sulphurized films were characterized by a variety of techniques and the results correlated with the synthesis conditions. To the best of our knowledge there are no available reports on the growth of CTS thin films by electrodeposition of Cu-Sn precursors using the two-electrode configuration, followed by soft annealing and sulphurization.

2. Materials and Methods

ITO conducting glass substrate was cut into the desired dimension of (1cm x 2 cm) and used as the working electrode and a graphite plate as a counter electrode. The ITO glass substrate was ultrasonically cleaned with acetone, subsequently with ethanol and deionized water.

The reagents used for the deposition of the Cu layer were 0.24 M copper sulphate pentahydrate ($CuSO_4.5H_2O$) as the source of copper metal ions and 1.36 M tri-sodium citrate ($Na_3C_6H_5O_7$) as a complexing agent. The electrolyte mixture was prepared by mixing 40 ml of $CuSO_4.5H_2O$ and 40 ml of $Na_3C_6H_5O_7$ in the electrochemical cell. The pH was reduced to 3.00 by drop-wise addition of 1.0 M $C_4H_6O_6$ (tartaric acid).

The electrolyte composition for the electrodeposition of Sn consisted of 0.55 M of $SnCl_2.2H_2O$ serving as a source of tin ions; 1.00 M of $C_6H_{14}O_6$ was used to improve layer stability

and adhesion of Sn and serve as a complexant and 2.25 M of NaOH was used as pH adjuster. An alkaline Sn electrolyte solution was used to deposit Sn films because an acid solution will dissolve the copper layer. The working solution was prepared by mixing the same volume (~30 ml) of $SnCl_2.2H_2O$ and $C_6H_{14}O_6$ in the electrochemical cell and the pH adjusted to 12.00 using NaOH.

All precursor chemicals were acquired commercially and used without further purification.

2.1. Deposition of the metal precursors

The sequential layer deposition (or the stacked elemental layer (SEL)) method was used to deposit the metallic precursors because it is easier to control the composition [33]. A two-electrode cell configuration was used with ITO coated glass substrate as the working electrode (cathode). A graphite plate was used as the counter electrode (anode).

Prior to electrodeposition of the metal precursors, an ER 466 Edaq computerized potentiostat system was used to perform cyclic voltammetry (CV) on the individual electrolyte solutions to determine deposition potentials for the metallic elements of interest. Electrodeposition of each metal layer was carried out at these predetermined potentials. The optimized deposition potentials were obtained as, -1.6 V for Cu and -1.8 V for Sn respectively.

Copper was first deposited because it has a more positive standard redox potential than tin. However, the adhesion of copper unto the glass substrates was a challenge. Copper easily rubs off and it peels off from the substrate when transferred into the Sn deposition solution. Thus there was the need to carry out a surface treatment described by Li et al. [34] which promotes better adhesion of copper onto the ITO glass substrate. This reduction process was carried out in a solution of 0.1 M H_2SO_4. According to Scragg et al. [29], the ITO substrate, modified by this electrolysis reduction process would have a monolayer of low valence of SnO_x forming on their surface. The deposited Cu atoms would then form a much stronger bond with Sn (II), which would contribute to improve adhesion of copper. It is also worth mentioning that, Cu/Sn is acknowledged as the optimal sequence to obtain high performance of the CTS solar cells [34, 35]. This sequence benefits from good metal exchange and stabilization of the metal layers [36, 37].

After the deposition of the Cu layer on the ITO substrate, the Sn layer was subsequently electrodeposited to form the Cu-Sn precursor. Between each deposition, the electrodeposited film was tested for adhesion by subjecting it to a continuous flow of deionized water. The stacked Cu-Sn metallic layers were kept in a desiccator to dry before annealing and characterization.

2.2. Soft annealing of Cu-Sn metal precursors and sulfurization

Low-temperature annealing, also called soft-annealing, of the stacked precursors prior to sulfurization has produced high efficient devices through a better mixing of the elemental stack to form precursor alloys [38].

Prior to soft annealing, the tube furnace was purged for 10 minutes with argon gas to ensure minimal oxygen in the tube. The stacked Cu-Sn precursor was then placed in the tube furnace and heated to a temperature of ~ 350 ^{0}C, and maintained at this temperature for 30 minutes. This temperature was held for a period of 30 minutes to improve intermixing of the elements Cu-Sn by alloying. Secondly this low temperature annealing may also dry the electrodeposited stack precursors from the remaining water and prevent the occurrence of cracks during high temperature annealing in sulphur. After 30 minutes the furnace was switched off and allowed to cool down under the flow of argon.

To obtain the CTS films, the alloy precursors were annealed in a saturated sulphur atmosphere. The instrumentation and the sulphurization method were the same as described in previous works [39, 40]. The sulphurization temperatures used were 500 ^{0}C and 550 ^{0}C for a duration of 1 hour.

2.3. Thin Film Characterization

The optical properties were measured using UV-VIS mini 1240 Spectrophotometer within the wavelength range of 300 - 1100 nm, a step height of 0.3 nm and a scan rate of 5 nm per second. The XRD patterns were obtained using an X-ray diffractometer with a Cu-kα radiation of wavelength 1.5406 Å. Samples were scanned in the 2θ range of 10 to 90^0. The machine was operated at 40 mA and 45 kV for phase analysis using the Bragg-Brentano geometry. A Phenom

instrument with nominal electron beam voltages of 15 kV, integrated with an EDAX equipment was used to determine the morphology and composition of the films.

3. Results and Discussions

3.1. X-Ray Diffraction Analysis

Fig. 1(a) shows the diffraction pattern of the blank ITO substrate. The peaks confirm the presence of tin (IV) oxide [JCPDS # 98-015-7451] which is one of the major constituents of the ITO substrate.

The XRD pattern of the soft-annealed elemental layers shown in Fig. 1(b), appears to be Sn-rich. Most of the peaks are assigned to Sn_3O_4 (00-020-1293) and Sn (01-085-6611). A few peaks are also assigned to the binary compound Cu_5Sn_6 (98-010-6530), which is an intermetallic compound phase easily formed when Sn is in contact with Cu, especially at elevated temperature (Zhang et al., 2014).

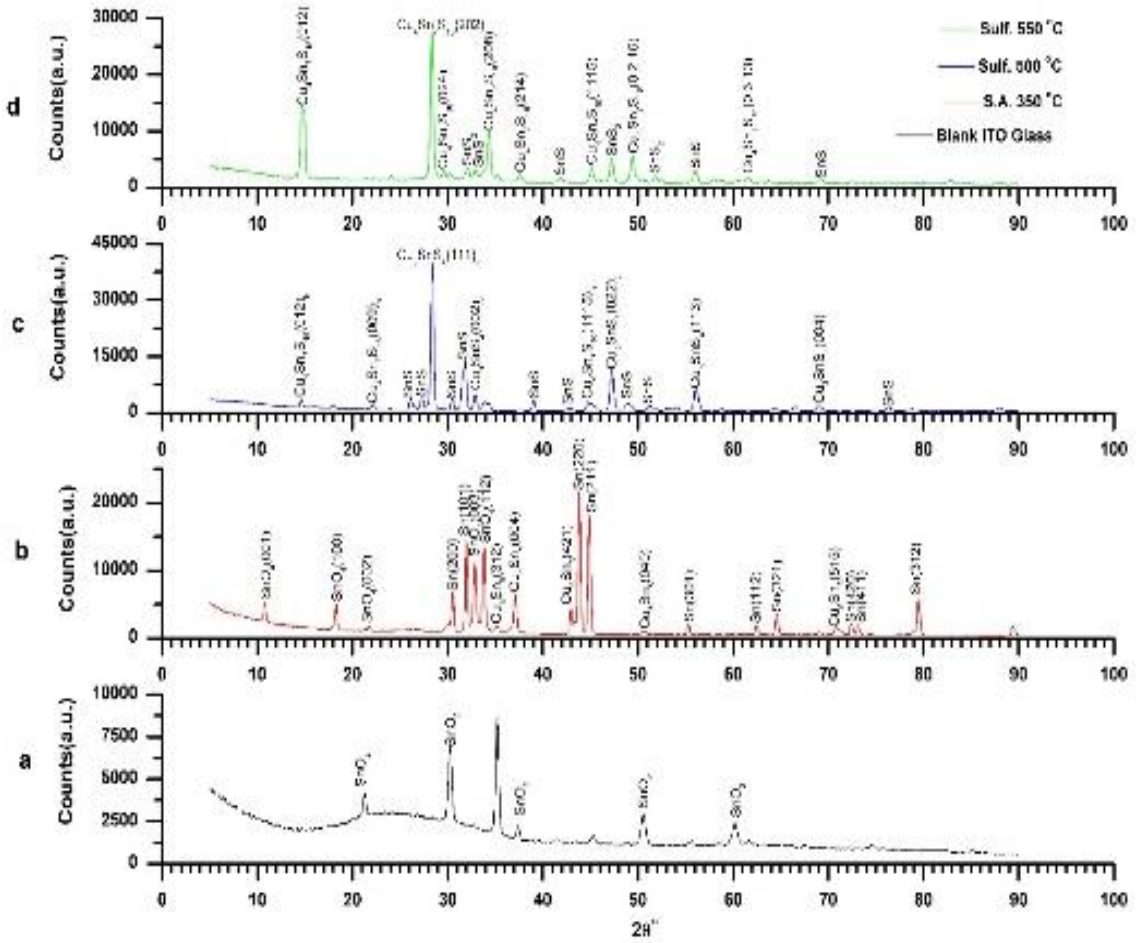

Fig. 1. XRD patterns a) ITO substrate b) soft annealed elemental stack c) CTS film obtained at a sulphurization temperature 500 ^{0}C d) CTS film obtained at a sulphurization temperature 550 ^{0}C.

The XRD patterns of the CTS thin films obtained at a sulphurization temperature of 500 ^{0}C (Fig. 1(c)) exhibits diffraction peaks indexed to SnS (98-065-1025), cubic $Cu_2Sn_3S_7$ (98-004-3532) and hexagonal $Cu_4S_{16}Sn_7$ (98-015-4696) phases. The majority phase can be clearly identified as cubic Cu_2SnS_3. The films exhibit a high intensity peak at 2θ value of 28.404°, suggesting a preferred growth in the (111). A confirmation of the composition of the deposit is shown in Table 1.

Table 1. Pattern list for the CTS film obtained at a sulphurization temperature of 500 ^{o}C.

Visible	Ref. Code	Score	Compound Name	Displ.[°2θ]	Scale Fac.	Chem. Formula
*	98-004-3532	53	Copper Tin Sulphide (2.67/1.33/4)	0.000	0.634	$Cu_{2.666}\ S_{3.999}\ Sn_{1.333}$
*	98-065-1025	44	Herzenbergite	0.000	0.259	S_1Sn_1
*	98-015-4696	33	Tetracopper(I) Heptatin(IV) Sulphide	0.000	0.424	$Cu_4S_{16}Sn_7$

There are several reports suggesting the coexistence of mixed phases in CTS films. Several authors have offered explanations on various factors which could influence the CTS structure formation. According to Lokhande et al. [2], the Cu/Sn elemental ratio is a major factor. Cu rich composition can form CuS, Cu_2S, Cu_3SnS_4 and Cu_4SnS_4 phases while the Cu poor composition can promote SnS, SnS_2, and $Cu_4Sn_7S_{16}$ phase formation. A report by Dahman and Mansour [22] suggests thin films obtained by sulphurization of Cu/Sn stacked precursors at the temperatures 450 ^{0}C, 500 ^{0}C, 550 ^{0}C and 580 ^{0}C exhibited XRD peaks attributable to CTS with cubic, monoclinic and/or tetragonal structures. According to Lemoine et al. [41], the $Cu_4Sn_7S_{16}$ phase is stable up to ~891 K. In line with these suggestions, the structure of the CTS films obtained in this work could be attributed to both the Cu/Sn elemental ratio and the sulphurization temperature.

Fig. 1(d) shows XRD pattern for the alloy precursor sulphurized at 550 ^{0}C. The pattern of prominent peaks is assigned to the hexagonal-$Cu_4S_{16}Sn_7$ phase. There is no evidence of other phases of CTS present in the film, suggesting that the Hexagonal $Cu_4Sn_7S_{16}$ phase, is chemically stable up to this temperature. There is a reduction in the number and intensity of peaks assigned to secondary phase, SnS, indicating an improvement in CTS purity at the higher sulfurization temperature [42]. The presence of several diffraction peaks shows that the CTS film is polycrystalline. The ITO phase peaks cannot be observed in the diffractograms of Fig. 1(c) and 1(d) indicating that the deposits had good coverage on the substrate.

A confirmation of the composition of the deposit is shown in Table 2.

Table 2. Pattern list for the CTS film obtained at a sulfurization temperature of 550 ^{0}C.

Visible	Ref.Code	Score	Compound Name	Displ.[°2θ]	Scale Fac.	Chem. Formula
*	01-079-4819	37	Tin Sulphide	0.000	0.293	SnS_2
*	98-004-3409	38	Tin Sulphide	0.000	0.749	S_1Sn_1
*	98-015-4696	65	Tetracopper(I) Heptatin(IV) Sulphide	0.000	0.640	$Cu_4S_{16}Sn_7$

The thermal stability/instability of the $Cu_4Sn_7S_{16}$ phase are new information that scientific community have to take into account for potential high temperature applications, especially in thermoelectricity [41].

3.2. Average grain size

The crystallite size (D) of the sample can be estimated according to the Scherrer's equation [43] as shown in equation (1):

$$D = \frac{0.9\lambda}{\beta cos\theta} \quad (1)$$

where λ is the X-ray wavelength and β is the FWHM of the most intense peak and θ is the corresponding Bragg diffraction angle. The estimated crystallite sizes are 27.60 and 26.68 nm for the films sulphurized at 500°C and 550 °C respectively.

3.3. Morphology and elemental analyses

The SEM micrographs and EDAX of the soft annealed elemental stack and sulphurized Cu-Sn alloy precursors are shown Fig. 2, 3, 4, and 5. The SEM image in Fig. 2(a) shows a compact, homogenous and smooth surface with good coverage over the entire substrate.

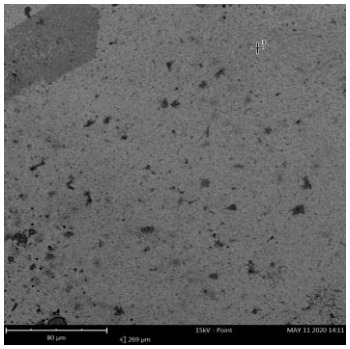

Fig. 2. (a) SEM image of the Cu-Sn elemental stack, soft-annealed at 350 ^{0}C in argon for 30 min.

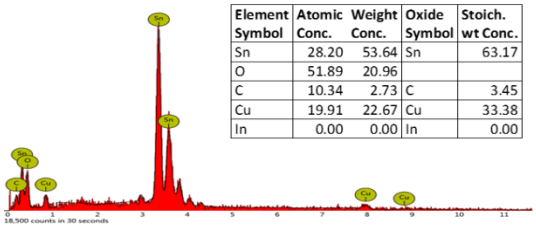

Element Symbol	Atomic Conc.	Weight Conc.	Oxide Symbol	Stoich. wt Conc.
Sn	28.20	53.64	Sn	63.17
O	51.89	20.96		
C	10.34	2.73	C	3.45
Cu	19.91	22.67	Cu	33.38
In	0.00	0.00	In	0.00

Fig. 2 (b) EDAX spectrum and chemical composition values of Cu-Sn precursor soft annealed at 350 ^{0}C in Argon for 30 minutes.

EDAX spectrum shown in Fig. 2b is consistent with the formation of the binary compound Cu-Sn. From the table inset, showing the chemical composition values, it is obvious that the soft annealed elemental stack is Cu poor. This might have influenced the CTS structure formation.

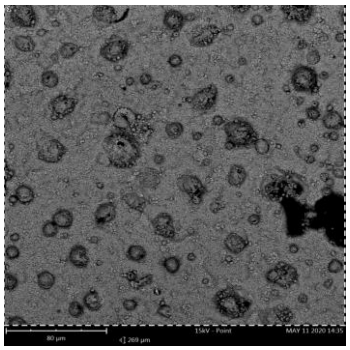

Fig. 3. (a) SEM micrograph of the CTS film obtained at a sulphurization temperature of 500 ^{0}C.

The morphology is compact and has the appearance of a molten matrix spread over the entire substrate, with some large grains embedded in it as shown in Fig. 3(a).

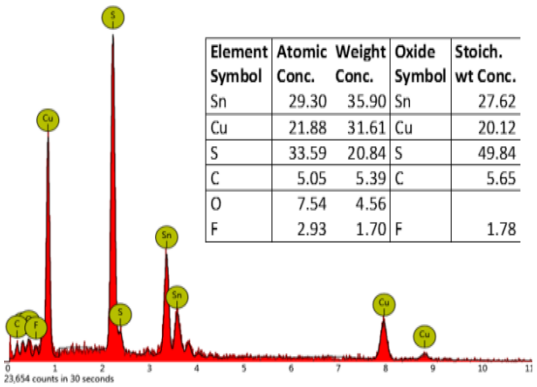

Element Symbol	Atomic Conc.	Weight Conc.	Oxide Symbol	Stoich. wt Conc.
Sn	29.30	35.90	Sn	27.62
Cu	21.88	31.61	Cu	20.12
S	33.59	20.84	S	49.84
C	5.05	5.39	C	5.65
O	7.54	4.56		
F	2.93	1.70	F	1.78

Fig. 3. (b) EDAX spectrum and chemical composition values of the CTS film obtained at a sulphurization temperature of 500 ^{0}C.

The EDAX in Fig. 3(b) clearly shows that the composition of the film is a mixture of Cu, Sn and S. The other elements such as O, F, **C** and they may emanate from the electrolyte solutions and the substrate.

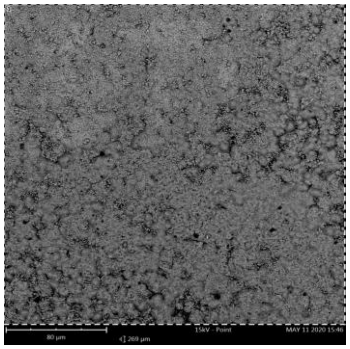

Fig. 4(a) SEM micrograph of the CTS film obtained at a sulphurization temperature of 550 ^{0}C.

The SEM image of Fig. 4(a) appears to be more uniform and fine grained than that Fig. 3(a). It also has good coverage over the entire substrate.

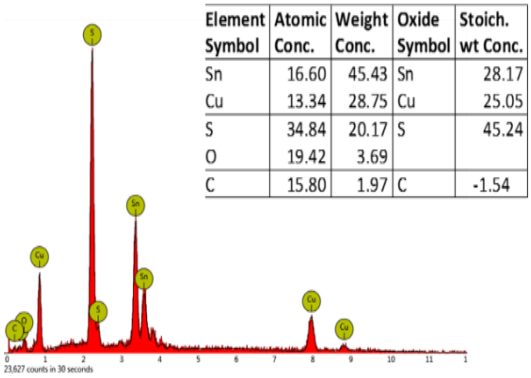

Element Symbol	Atomic Conc.	Weight Conc.	Oxide Symbol	Stoich. wt Conc.
Sn	16.60	45.43	Sn	28.17
Cu	13.34	28.75	Cu	25.05
S	34.84	20.17	S	45.24
O	19.42	3.69		
C	15.80	1.97	C	-1.54

Fig. 4. (b) EDAX spectrum and chemical composition values of the CTS film obtained at a sulphurization temperature of 550 ^{0}C.

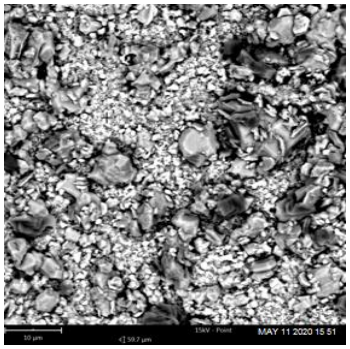

Fig. 5. SEM image (with larger magnification) of CTS thin films obtained after sulphurizing at 550 ^{0}C.

The micrograph in Fig. 5, shows a compact, homogenous morphology, few pinholes with well-defined densely packed grains of different shapes and dimensions. There are clearly distinguishable hexagonal shaped grains at the bottom left corner of the micrograph.

3.4. Optical band gap of the CTS Film

The nature of the optical transition, whether direct or indirect and the band gap value can be obtained from the equation (2) as given by Stern (1963) and cited in Anuar et al. [44].

$$A = \frac{[k(h\upsilon - E_g)]^{n/2}}{h\upsilon} \quad (2)$$

where A, is the absorbance, υ is the frequency, *h* is the Planck's constant, *k* is a constant and *n* can take the value of 1 or 4 based on whether the transition is a direct transitions or indirect transitions. CuS, and SnS are all direct band gap materials. Thus, we assume that their mixed compositions would also have a direct band gap and hence, n = 1.

The band gap energy is obtained by plotting a line of best fit on the $(Ahv)^{2/n}$ versus *hv* graph and extrapolating the line to intersect the energy axis at $(Ahv)^{2/n} = 0$ as shown in Fig. 6.

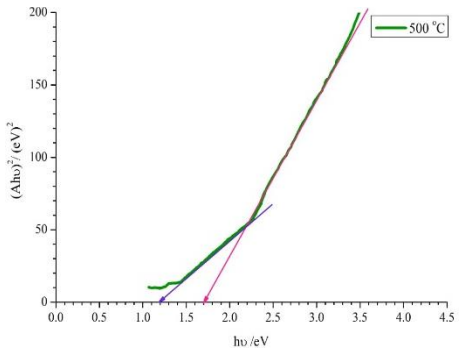

Fig. 6 A graph of $(Ahυ)^2$ plotted as a function of the photon energy, hυ for CTS thin film sulphurized at 500 ^0C.

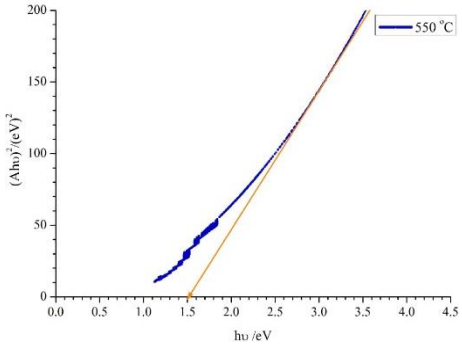

Fig. 7. A graph of $(αhυ)^2$ plotted as a function of the photon energy, hυ for CTS thin film sulfurized at 550 ^0C.

In Fig. 6, extrapolations of the curves to the energy axis for zero absorption show the presence of two energy gaps; a lower one at 1.2 eV, and a higher one at 1.7 eV. These two band gaps may be as a result of the coexistence of several phases within the sample. Fig. 7, shows only one band gap with a value of 1.5 eV which falls within the range of 0.93 to 1.77 eV, reported for CTS, depending on the preparation conditions [45].

4. Conclusions

CTS thin films have been successfully synthesized by electrochemical deposition of Cu-Sn precursor, using a two-electrode configuration for the first time, followed by soft annealing and sulphurization. The growth of the CTS samples was achieved by sequential deposition of the metal layers in the order ITO|Cu|Sn, using a two-electrode electrochemical cell, with graphite plate as the counter electrode. The elemental layers were soft annealed in argon at 350 ^0C, followed by sulphurization at two different temperatures, 500 ^0C and 550 ^0C. The structural, morphological, compositional and optical properties of the films have been investigated in detail. The XRD analysis of the soft annealed samples had most of the peaks assigned to Sn_3O_4 and Sn. A few peaks were also assigned to the binary compound Cu_5Sn_6, The CTS thin films obtained at a sulphurization temperature of 500 ^0C showed the coexistence of SnS, Cubic $Cu_2Sn_3S_3$ and hexagonal $Cu_4S_{16}Sn_7$ phases.

The majority phase was clearly identified as cubic Cu_2SnS_3 with (111) preferential orientation. For the films sulphurized at 550 ^0C, the major peaks were indexed to the hexagonal-$Cu_4S_{16}Sn_7$ phase, with preferred orientation along the (202) plane. There was no evidence of other phases of CTS present in the film, suggesting that the hexagonal $Cu_4Sn_7S_{16}$ phase, is chemically

stable up to this temperature. There were relatively fewer low intensity peaks assigned to the secondary phase, SnS, indicating an improvement in CTS purity at the higher sulphurization temperature. All the CTS films were polycrystalline. SEM images of the CTS films show a compact, homogenous morphology, with densely packed grains. The films sulphurized at 550 ^{0}C, showed better homogeneity. EDAX spectra of the sulfurized alloy precursors were consistent with the formation of CTS. Optical analysis show the CTS films exhibit a direct band gap.

The film obtained at the lower sulphurization temperature had two band gaps as a consequence of the mixture of phases present in the sample. The film obtained at the higher sulphurization temperature had an energy band gap of 1.5 eV, which falls within the range of values reported in literature. The present work can provide a new synthesis route for the preparation of CTS thin film for device applications.

Acknowledgements

The authors wish to acknowledge the department of Physics and Earth Science, University of Ghana, Legon for allowing us to use their XRD and SEM/EDS machines and CSIR for their expertise in glass blowing**.** We acknowledge the provision of instrumentation in the Dept. of Physics and Chemistry, KNUST.

References

[1] S. Yasar, S. Kahraman, S. Çetinkaya, I. Bilican, Journal of Alloys and Compounds **618**, 217 (2015).
[2] A. C. Lokhande, P.T. Babar, V. C. karade, M. G. Gang, V. C. Lokhande, C. D. Lokhande J. H. Kim, Materials Chemistry A. **7**, 17118 (2019).
[3] P. Zawadzki, L.L. Baranowski, H. Peng, E.S. Toberer, D.S. Ginley, W. Tumas, S. Lany, Applied Physics Letters **103**(2), 53902 (2013).
[4] M. Onoda, X. Chen, A. Sato, H. Wada, Materials Research Bulletin **35**, 1563 (2000).
[5] A. Amlouk, K. Boubaker, M. A. Vacuum **85**(1), 60 (2010).
[6] S. Dias, B. Murali, S. B. K. Mater. Chem. Phys. **167**, 309 (2015).
[7] J. Han, Y. Zhou,Y. Tian, Z. Huang, X. Wabg, J. Zhong, Z. Xia, Frontiers of Optoelectronics **7**, 37 (2014).
[8] U. V. Ghorpade, M.P. Suryawanshi, S.W. Shin, I. Kim, S.K. Ahn, J.H. Yun, C. Jeong, S. S. Kolekar, J. H. Kim. Chem. Mater. **28**(10), 3308 (2016).
[9] C. Wu, Z. Hu, C. Wang, H. Sheng, J. Yang, Y. Xie, Applied Physics Letters **91**(14), 143104 (2007).
[10] Z. Pan, K. Zhao, J. Wang, H. Zhang, Y. Feng, ACS Nano **7**, 5215 (2013).
[11] H. B. Michaelson, Journal of Applied Physics **48**(11), 4729 (1977).
[12] D. M. Berg, R. Djemour, L. Gütay, G. Zoppi, S. Siebentritt, P. J. Dale, Thin Solid Films **520**(19), 6291 (2012).
[13] M. Bouaziz, J. Ouerfelli, S.K. Srivastava, J.C. Bernède, M. Amlouk, Vaccum ***85***(8), 783 (2011).
[14] H. Zhang, M. Xie, S. Zhang, Y. Xiang, Journal of Alloys and Compounds **602**, 199 (2014).
[15] K. Lohani, E. Isotta, N. Ataollahi, C. Fanciulli, A. Chiappini, P. Scardi, Journal of Alloys and Compounds **830**, 154604 (2020).
[16] B. Pejjai, V. R. M. Reddy, S. Gedi, C. Park, Journal of Industrial and Engineering Chemistry **60**, 19 (2018).
[17] A. Lokhande, R. Chalapathy, M. He, E. Jo, M. Gang, S. Pawar, C. Lokhande, J. H. Kim, Solar Energy Materials and Solar Cells **153**, 84 (2016).
[18] T. A. Kuku, O. A. Fakolujo. Solar Energy Materials **16**(1–3), 199 (1987).
[19] M. Umehara, S. Tajima, Y. Aoki, Y. Takeda, T. M. Appl. Phys. Express *9*(7), (2016).

[20] P. A. Fernandes, P. M. P. Salomé, A. F. da Cunha, Journal of physics D: Applied Phyics **43**, 21 (2010).
[21] U. Chalapathi, Y. Jayasree, S. Uthanna, V. Sundara Raja. Physica Status Solidi (A) **11**(210), 2384 (2013).
[22] S. R. H. Dahman, A. Alyamani, L. El Mir, Vacuum **101,** 208 (2014).
[23] M. T. S. Nair, C. Lop ez-Mata, O. GomezDaza, P. K. Nair. Semiconductors Science Technology **18**, 755 (2003).
[24] H. Soonmin. International Journal of Research in Engineering and Innovation **1**(6), 143 (2017).
[25] V. Robles, J. F. Trigo, C. Guillén, J. Herrero. Journal of Alloys and Compounds **642**, 40 (2015).
[26] N. R. Mathews, M. Pal, L. Huerta, J Mater Sci: Mater Electron **24**, 4060 (2013)
[27] C. J. Hibberd, E. Chassaing, W. Liu, D. B. Mitzi, D. Lincot, A. N. Tiwari, Progress in Photovoltaics: Research and Applications **18**(6), 434 (2010).
[28] E. M. Mkawi, M. K. M. Ali, A. S. Mohamed, K. Ibrahim, M. A. Farrukh. Journal of Materials Science:Materials in Electronics **25**(2), 857 (2013).
[29] J. J. Scragg, T. Ericson, T. Kubart, M. Edo, C. Platzer-bj. Chemistry of Materials **46**, 25 (2011).
[30] S. Ahmed, K. B. Reuter, O. Gunawan, L. Guo, L. T. Romankiw, Advanced Energy Materials **20**, 1 (2011).
[31] Y. Shen, C. Li, R. Huang, R. Tian, Y. Ye, L. Pan, K. Koumoto, R. Zhang, C. Wan, Y. Wang, Sci. Rep. **6**, 32501 (2016).
[32] O. K. Echendu, K. B. Okeoma, C. L. Oriaku, I. M. Dharmadasa, Advanced Material Science Engineering **2016**, 3581725 (2016).
[33] F. Jiang, S. Ikeda, Z. Tang, T. Minemoto, W. Septina, Prog. Photovolt: Res. Appl. **23**, 1884 (2015).
[34] J. B. Li, V. Chawla, B. M. Clemens. Advanced Materials **24**(6), 720 (2012).
[35] S. Ahmed, K. B. Reuter, O. Gunawan, L. Guo, L. T. Romankiw, H. Deligianni, Advanced Energy Materials **2**(2), 253 (2012).
[36] X. He, H. Shen, W. Wang, J. Pi, Y. Hao, X. S. Applied Surface Science **282**, 765 (2013).
[37] J. J. Scragg D. M. Berg, P. J. Dale. Journal of Electroanalytical Chemistry **646** (1-2), 59 (2010).
[38] S. M. Lee, S. Ikeda, T. Yagi, T. Harada, A. Ennaoui, M. Matsumura, Physical Chemistry Chemical Physics **13**(14), 6662 (2011).
[39] E. A. Botchway, F. K. Ampong, I. Nkrumah, F. Boakye, R. K. Nkum, Open Journal of Applied Sciences **9**, 725 (2019).
[40] M. Paal, I. Nkrumah, F. K. Ampong, D. U. Ngbiche, R. K. Nkum, F. Boakye, Science Journal of University of Zakho ***8***(3), 97 (2020).
[41] P. Lemoine, C. Bourgès, T. Barbier, V. Nassif, S. Cordier, E. Guilmeau, Journal of Solid State Chemistry **247**, 83 (2017).
[42] Z. Tong, C. Yan, Z. Su, F. Zeng, J. Yang, Y. Li, L. Jiang, Y. Lai, F. Liu, Appl. Phys. Lett. Journal of Materials Chemistry A **105**(223903), 125 (2014).
[43] C. K. Bandoh, I. Nkrumah, F. K. Ampong, R. K. Nkum, F. Boakye, Chalcogenide Letters **18** (2), 81, (2021).
[44] K. Anuar, W. Tan, M. Jelas, S. M. Ho, S. Y. Gwee, Thammasat Int. J. Sc.Tech. **15**(2), 64 (2010).
[45] S. A. Vanalakar, G. L. Agawane, A. S. Kamble, C. W. Hong, P. S. Patil, J. H. Kim, Solar Energy Materials and Solar Cells **138**, 1 (2015).